Received April 14, 2020, accepted May 1, 2020, date of publication May 6, 2020, date of current version May 20, 2020.
Digital Object Identifier 10.1109/ACCESS.2020.2992645

Deep Learning Assisted Predict of Lung Cancer on Computed Tomography Images Using the Adaptive Hierarchical Heuristic Mathematical Model

HENG YU, ZHIQING ZHOU, AND QIMING WANG
School of Information Engineering, Pingdingshan University, Pingdingshan 467000, China
Corresponding author: Zhiqing Zhou (2544@pdsu.edu.cn)

ABSTRACT Lung cancer is known to be one of the most dangerous diseases which are the main reason for disease and death when diagnosed in primitive stages. Since lung cancer can only be detected more broadly after it spread to lung parts and the occurrence of lung cancer in the earlier stage is very difficult to predict. It causes a greater risk as radiologists and specialist doctors assess the existence of lung cancer. For this reason, it is important to build a smart and automatic cancer prediction system that is accurate and at which stage of cancer or to improve the accuracy of the previous cancer prediction that will help determines the type of treatment and treatment depth depending on the severity of the disease. In this paper, the Adaptive Hierarchical Heuristic Mathematical Model (AHHMM) has been proposed for the deep learning approach. To analyze deep learning based on the historical therapy scheme in the development of Non-Small Cell Lung Cancers (NSCLC) automated radiation adaptation protocols that aim at optimizing local tumor regulation at lower rates of grade 2 RP2 radiation pneumonitis. Furthermore, the system proposed consists of several steps including acquiring the image, preprocessing, binarization, thresholding, and segmentation, extraction of features and detection of deep neural network (DNN). Segmentation of the lung CT image is carried out to extract any significant feature of a segmented image, and a specific feature extraction method is implemented. The test evaluation showed that the model proposed could detect 96.67 % accuracy of the absence or presence of lung cancer.

INDEX TERMS Lung cancer detection, deep learning, deep neural network, mathematical model.

I. INTRODUCTION

A malignant tumor labeled by uncontrolled cell growth in lung tissues is lung cancer, known as lung carcinoma [1]. This must be treated so that its growth is not spread to other parts of the body employing metastases [2], [3]. Carcinoma is the majority of cancers starting in the lung the two main types are carcinoma of small cells of lung and non-small cells [4] of the lung the primary factor in 88% of lung cancers is long-term smoking. Approximately 15–20 % of cases occur in humans [5] who has not smoked except because of asthma, smoking, asbestos and radon gas. The traditional method to predict the presence of lung cancer is computer tomography (CT) and X-rays [6], [7]. Biopsy, which is usually performed with a bronchoscope or a CT scan, confirms the diagnosis. The impact of death due to cancer in men is due primarily to lung cancer [8] and a new and comprehensive approach to the early diagnosis of lung cancer should, therefore, be established [9]. The method of image recognition has been enhanced by the recent technology in deep learning or deep neural networks. Scan the pattern in an image utilizing Deep Neural Networks and decide if it recognizes the pattern [10]. Besides, it is look for several patterns when analyzing an image. Neural network training requires a predetermined dataset to be used by the network to recognize, learn and classify a picture [11], [12]. DNN has become more and more common because it can easily be used for recognizing image patterns and classifying images [13]. Figure 1(a) shows the nodule segmented from the original CT scan image. Figure 1(b) shows the Pulmonary nodule with a chest CT image [14].

Most of the patients with non-small-cell lung cancer (NSCLC) [16] are obsolete because of locally improved diseases or remote metastases and therefore radiation treatment

The associate editor coordinating the review of this manuscript and approving it for publication was Wei Wei.

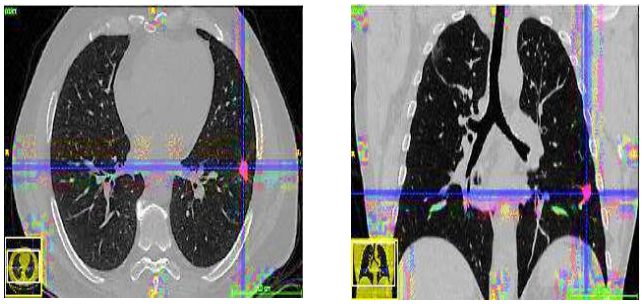

1(a) 1(b)

FIGURE 1. (a) Nodules segmented from the original CT scan image (b) Pulmonary nodule with chest CT image [15].

remains the prime choice to treat them [17]. However, following important technological advances in radiation preparation and imaging, the treatment results remain very low [18]–[20]. It is believed that the rise in radiation is an option for improving the results of the treatment [21]. Radiation therapy is effective for treating carcinogenicity can pose the risks that have to be changed according to the characteristics of each patient [22]. The risk of exposure from chest irradiation leading to radiation-induced pneumonitis (RP) is one of the major restrictions for lung cancer care. RP induces fever, cough, etc. and cause patients' quality of life, even though local tumor control (LC) is ensured [23]–[26].

In this paper, DNN can be used in the various medical field to extract features and classify images. The Deep Neural Network model has been trained and tested using functional Computed Tomography (CT) data. The images has been divided into one convolutional layer only. A comparative study analyzes how the variable affects the formation procedures of a Deep Neural Network to identify lung cancer images. It is difficult to classify for' heavier' images with DNN. While images of the form CT are used primarily in medical imaging, unnecessary artifacts can be created. The threshold has been used to prevent the images from displaying these objects. The threshold procedure eliminates unwanted peaks in pixels of the medical image of lung cancer.

The main contributions of the paper are,

- To propose the Adaptive Hierarchical Heuristic Mathematical Model (AHHMM) to predict lung cancer based on Deep learning using computed tomography images.
- Designing the deep neural network (DNN) framework to extract high-level features directly from the information and applying the K-means clustering algorithm.
- The experimental results has been performed to enhance the accuracy in prediction and the dataset http://diagnijmegen.nl/index.php/Lung_Cancer has been utilized.

The remainder of the paper decorated as follows: section 1 and section 2 discussed the background and introduction of lung cancer detection and existing methods. In section 3 the adaptive hierarchical heuristic mathematical model for lung cancer detection has been proposed. In section 4 the experimental results has been demonstrated. Finally, section 5 concludes the research article.

II. RELATED SURVEY

Jakimovski and Davcev [27] proposed the Double convolutional deep neural network (DCDNN) for lung cancer stage prediction. In the training of both the CDNN and the regular CDNNs, they used Computed Tomography (CT) scans. These topologies have been experimented against images of pulmonary cancer to assess the stage of tx cancer in that topologies can predict lung cancer. The first phase involved the pre-classification of CT images from the first dataset to concentrate on CDNN research. Next, they create the double deep neural network Convolution with max pool, to carry out a more comprehensive search. They eventually utilized Computed Tomography scans of various stage Tx cancer of lung cancer to establish the Tx level where CDNN detects lung cancer potential. The findings are reviewed with the medical doctors of the oncology department and are deemed sufficient to detect cancer in T3. This technique is used by doctors for early detection and early treatment.

Nasser and Abu-Naser [28] introduced the Artificial Neural Network (ANN) for detecting lung cancer. A Network for the Prediction of the Absence or Presence of Lung Cancer in the Human Body was developed. Symptoms like yellow fingers, anxiety, chronic illness, weariness, allergy, wheezing, roar, breath shorter, swallowing difficulty and chest pain were used to diagnose lung cancer. Symptoms like yellow fingers. They were used as input variables for our ANN and other details about the human. trained and validated data collection entitled' survey cancer of the lung.' The system evaluation showed that the ANN model would detect 96.67 percent accuracy in the absence or presence of lung cancer. They have carried out some planning and analysis to make the data more predictive.

Atsushi Teramoto *et al.* [29] suggested the Deep Convolutional neural network (DCNN) for automated classification of lung cancer from cytological pictures. The DCNN used for classification contains three convolutional layers, two fully connected layers, and three pooling layers. The DCNN has been equipped with its original database using a graphics processing unit during measurement experiments. Microscopic images were first trimmed and resampled to get pictures at the resolution of 256 to 256 pixels and collected images were increased by rotation, flipping, and filtering, to avoid unnecessary overfitting. The probabilities for the three types of cancers were calculated using the planned method. The results determined show approximately 72% of the images were correctly classified, which is consistent with cytotechnology and pathogens' precision. Thus, the scheme developed is useful when classifying microscopic lung cancers.

Shakeel *et al.* [30] initialized the Improved profuse clustering technique and deep learning instantaneously trained neural network (IPCT-DLITNN) for lung tumor prediction from CT images. Pre-processing lung cancer has become a

critical stage for improving the quality of the input picture, such as edge detection, pulmonary imaging, pulmonary imaging enhancement, and image denoisation. Image denoising is a crucial task preceding further picture preparation such as segmentation, surface exams, feature extraction and so on, which eliminates the noise and retains, to the extent possible, the edges and additional comprehensive characteristics. This paper focuses on enhanced pulmonary consistency and lung cancer diagnosis by minimizing error. The lung CT images are obtained using a weighted average histogram equalization method, which effectively eliminates noise from images and increases photo quality, and using an improved profuse clustering technique (IPCT) to segregate the area injured. The injured area has different spectral features.

To overcome the above survey, in this paper, the Adaptive Hierarchical Heuristic Mathematical Model (AHHMM) to predict lung cancer based on Deep learning using computed tomography images has been proposed. Lung cancer is an abnormal cell disease that multiplies and becomes a tumor. The lungs, or the lymph fluid that covers the lung tissue, can hold cancer cells away from the lungs. Deep learning is better known than conventional techniques for image classification. The clinical decision making for lung cancer has been carried out by the proposed mathematical model. The proposed method achieves high accuracy in the prediction of lung cancer cells.

III. ADAPTIVE HIERARCHICAL HEURISTIC MATHEMATICAL MODEL (AHHMM)

In this paper, the adaptive hierarchical heuristic mathematical model has been proposed for the recognition of lung tumors on CT pictures. In this study, the datasets has been taken from http://diagnijmegen.nl/. In a wide variable list, the Bayesian network technique has been used for graph theory to define the radiotherapy environment that allows the hierarchical links between variables and interest results to be recognized. The method used is based on the identification from a high-dimensional data set of separate extended Markov blankets (MBs) for RP2 and LC.

Case 1 (Deep Neural Network): Let's consider the data $\{y_j\}$ with labels $\{z_j\}$ such that $\chi = \{(y_j, x_j) \,|\, y_j \in \Re^m, z_j \in \Re^n, j = 1, \ldots M\}$ a DNN determines a function $f_{DNN} : \Re^m \to \Re^n$ to weave via data such that $f_{DNN}(y_j) \cong z_j$ as much as possible through the utility of 3 different parts: Neurons $x_j \in \Re$, layers of l neurons $x = (x_1, \ldots x_l)$ and activation function ρ, If a deep neural network has layers i = 0, ... k every of that has m_i neurons, then i = 0 and k would indicate the initial input and last output layer correspondingly. An activation function $\rho : \Re^{m_{i-1}} \to \Re^{m_i}$ links the neurons of (i-1)th layer $x^{(i-1)} \in \Re^{m_{i-1}}$ and those of the ith layer $x^i \in \Re^{m_i}$ would satisfy:

$$x^{(i)} = \rho(\Theta^{(i-1)} \cdot x^{(i-1)} + a^{(i-1)}) \quad (1)$$

As shown in equation (1) A typical option of ρ is a rectified linear unit (ReLU)or sigmoid. Where $\Theta^{(i-1)} \in \Re^{m_i \times m_{i-1}}$ and $a^{(i-1)} \in \Re^{m_{i-1}}$ denotes the unknown weights and bias to be calculated. Our better variables $\{\Theta^{(i)}, a^{(i)}\}_{i=0}^{k-1}$ are then derived from backward and forward propagation resulting from Deep Neural Network loss function,

$$L(\Theta, x, \lambda) = \frac{1}{2}\left\|z - x^k\right\|^2 - \sum_{i=1}^{k} \langle \lambda^{(i-1)}, x^{(i)} - \rho(\Theta^{(i-1)} \cdot x^{(i-1)} + a^{(i-1)}) \rangle \quad (2)$$

As shown in equation (2) where $\lambda^{(i-1)} \in \Re^{m_{i-1}}$ are the Lagrange multipliers at layer i-1 to protect layerwise data equation 1.

A. IMAGE-PREPROCESSING

Medical image processing methods have been used to predict changes present in the lungs of the recorded CT pulmonary images. The lung cancer processing structure is shown in Figure 2. Lung tumor has successfully been detected by the medical image processing technique according to the processing structure of the lung picture. The following section provides a detailed explanation of each processing phase. The images captured are examined in pixel noise prediction, contrasted details to improve the quality of the Computed Tomography pulmonary image, since the image captured contains several incohérent details, low pixel quality which decreases the accuracy of detected lung cancer. The pixel intensive testing process has been utilized that essentially changes the pixel picture interpretation, the accuracy of Computed Tomography lung image is increased. The current pixel shift removes the inconsistent pixel and the noise pixel. Image histogram methods are used for image quality enhancement because it works with better and simple on different images.

B. IMAGE-SEGMENTATION

The next major step is the segmentation of the region injured by cancer by the use of the K-mean algorithm using the enhanced lung CT image. The implemented segmentation approach inspects the pixel similarity in the lung CT images and divides the images into several sub-settings to predict the area concerned. Analysis of the image pixels in the image and group of same superpixels into a similar group for abrupt pixels detection. The pixel or information is subsequently tested during the image fragmentation process to predict the comparability of data using the same value of spectrum or pixels. The pixel similarity attribute involves the quantitative image evaluation used to accurately shape the cluster. The enhanced quality of the Lung Computed Tomography image pixels is tested and every pixel is considered as an element in the app. For parts of the affected region, an undirected graph is created.

C. IMAGE-CLASSIFICATION

The final stage is the identification of lung cancer through an explosion-trained deep learning neural network (DITNN). The image training should be carried out utilizing a deep-learning NN before the classification process is done since it does not need manual features. Alternatively, the deep learning process uses a captured segmented image or lung CT image that utilizes a huge number of hidden layers to identify

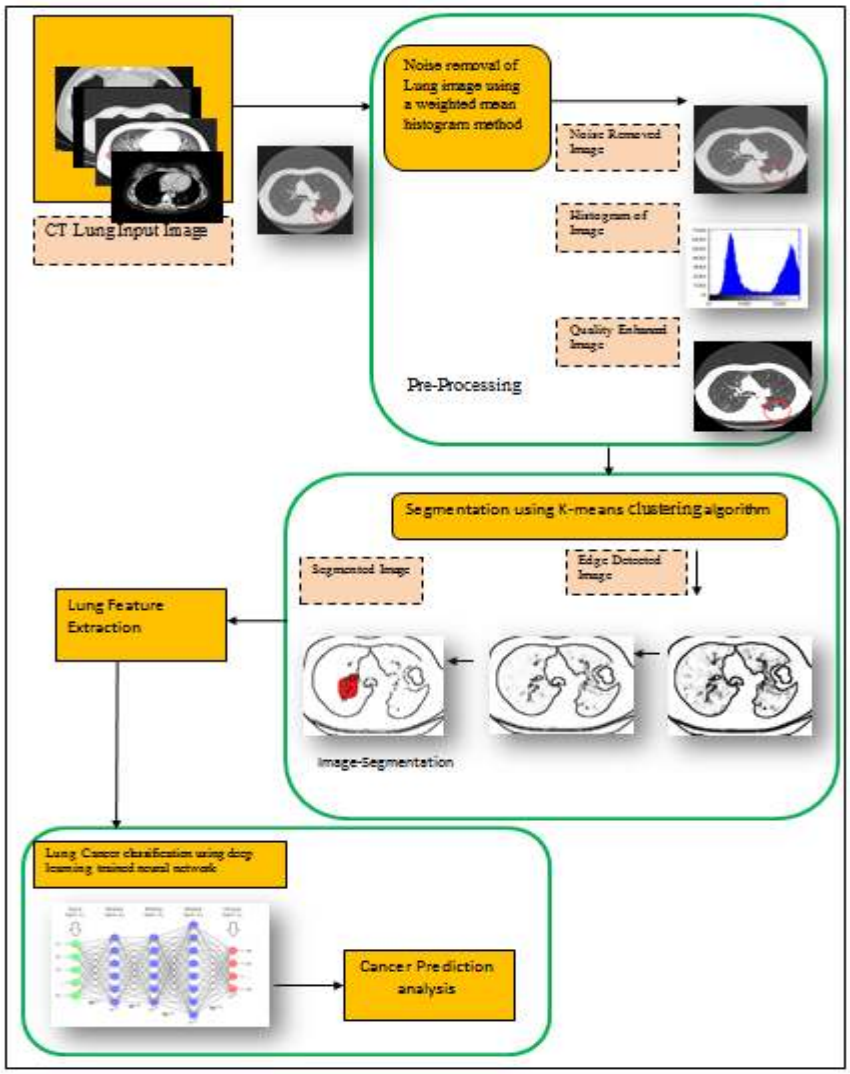

FIGURE 2. The architecture of proposed AHHMM method.

the boundaries of the image and the corresponding features utilized for the network's creation with a large amount of information.

Case 2 (Generative Adversarial Nets): Generative adversarial network (GANs) has been utilized to synthesize more radiotherapy-like information, to mitigate the issue of small sample size in datasets when modeling difficult state transitions in the circumstances of radiation. A GAN contains two neural networks, one generative (H). The other is biased (E), which seeks to test the (dis)-similarity of the condensed data against the actual data. In general, H is designed to generate inextricable data to confuse E, while E tries to differentiate between the data produced by H or not. In a competitive sense, they compete with each other, therefore the term GAN. The adversary E and H character are generated using the loss function of the mini-max two players:

$$\min_{H}\max_{E} L(H,E) = \min_{H}\max_{E} G_{y\sim Q_{data(y)}}[\log E(y)] + G_{x\sim Q_{prior(x)}}\left[\log\left(1-E\left(H\left(x\right)\right)\right)\right] \quad (3)$$

where $E(z) = \begin{cases} 1, & z \text{ is real} \\ \frac{1}{2} & z \text{ is indistinguishable} \\ 0, & z \text{ is generated}. \end{cases}$

1) DEEP Q NETWORKS

In reinforcement learning, there is a Markov decision process (MDP) and an agent. Reinforcement learning has been utilized to mimic how doctors deciding on the dose fraction tradeoff required to dictate to a patient. Over a decision made by present state $\pi : W \rightarrow B$ an agent acquires respective reward T and gets reinforced to the next state. An agent taking care of supplying tasks $b \in B$ in a condition, which is explained by the different states $w \in W$ in the conditions. The transition to state T is feedback for the agent to see how his further approach for future tasks could be optimized. A second opinion or the presence of a specialist in our setting would be an external agent. In the next phase of a dose-escalation radiotherapy therapy course, the required dose per fraction (adaptation) will be determined. This agent

interacts with the transitional DNN-rebuilt radiotherapy artificial environment (RAE) and adapts its strategy of adaptation to the feedback received.

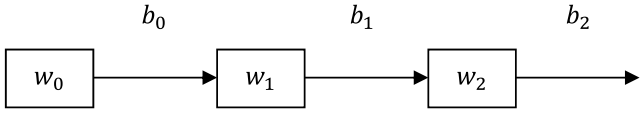

In Q-learning, the best policy $\pi^* : W \rightarrow B$ is stated such that $P^{\pi^*} = max_\pi P^\pi$ is achieved when the assess recurrence method is adapted for estimation. Through the equation of Bellman's off-policy, the calculation of optimal P^{π^*} is transformed into a repeated series stated as the following equation (4),

$$P^\pi(w,b) = G\left[\sum_{l=1}^{\infty} \delta^k T(w_l, \pi(w_l)) \,|\pi, w_0 = w, b_0 = b\right] \tag{4}$$

$$\widetilde{P}_{j+1}(w,b) = G_{r\sim Q_{wb}}\left[T(w,b) + \delta \max_{a\in B} \widetilde{P}_j(r,a)\right] \tag{5}$$

The convergence is meet at the single fixed point as $j \rightarrow \infty$ based on contraction mapping theorem,

$$\widetilde{P}^*(w,b) = G_{r\sim Q_{wb}}\left[T(w,b) + \delta \max_{a\in B} \widetilde{P}^*(r,a)\right] \tag{6}$$

To estimate the Q-function effectively utilizing supervised learning by DNN by $\widetilde{P}_j = P^{\Theta_j}_{DNN}$, where Θ_j indicates the weights of DNN in equation (1) at jth recurrence with a series of loss functions $\mathcal{L}_j(\Theta_j)$ to be reduced as following equation (7):

$$L_j(\Theta_j) = G_{(w,b)\sim\sigma}\left[\left(G_{r\sim Q_{wb}}\left[T(r,b) + \delta \max_{a\in B} P^{\Theta_{(j-1)}}_{DNN}(r,a)\right] - P^{\Theta_j}_{DNN}(w,b)\right)^2\right] \tag{7}$$

As shown in equation (7) where tasks b called behavior distribution and σ is the probability distribution over policy series w. The loss function (7) can be observed in Deep Neural Network series $\{P^{\Theta_j}_{DNN}\}$ such that $\{P^{\Theta_j}_{DNN}\}^{\infty}_{j=1} \rightarrow \{X_j\}^{\infty}_{j=1}$,

$$\mathcal{L}_j(\Theta_j) = G_{(w,b)\sim\sigma}\left[\left(Z_j(w,b) - P^{\Theta_j}_{DNN}(w,b)\right)^2\right] \tag{8}$$

Figure 3 demonstrates the training procedures of the deep learning approach. The trained features are stored in the database as models for the manual prediction of lung cancer-relevant to extraction features. The data is usually supported on 150 hidden layers. While the classification process, the extracted spectral features are categorized and self-trained using an immediately trained neural network. By adding the stored node when aiming at the lung features, the network uses the extracted functionality to operate according to the unsupervised classification method.

As shown in algorithm 1 the Modified K-means clustering algorithm has been proposed. On the data of the lung cancer modified K-means clustering algorithm has been utilized

Algorithm 1 Modified K-Means Clustering Algorithm

```
K-means
(attributes (m), priority (no of a cluster))
{
Sort (attributes.Priority);
For (j=1 to k)
{
Centroid [j]=findmean (C_j);
}
For (i=1 to k (k-1)/2)
{
Dis [i] =dis (centroid [1tok]);
Temp [i]=dis [i]/n;
}
Until (–m!=0)
{
Apply m to ploted points;
Shift +or -temp towards other centroid;
For (j=1 to k)
{
Centroid [j]=find
Mean (C_j);
}
For (i=1 to k (k-1)/2)
{
Dis [i]=dis (centroid [1 to k]);
Temp [i]=dis [i]/m;
}
}
}//end
```

and the datasets into Two groups of clusters: one cluster of lung cancer patients and the other for cancer-free patients. Based on the value of the attributes, the number of clusters is determined. For example, when the tumor size of the lung cancer dataset is greater than 3, the patient is likely to be affected by lung cancer. Two clusters are formed based on these plotted points and take two centroid points. The effect of the new attributes on the cluster is described as-if the next attribute is smoking, the cluster moves to either left or right to a certain distance, depending on the cluster's impact.

Case 3 (Radiotherapy Dose Adaption): A key objective of this research has to determine whether potentially can use reinforcement learning to regenerate previously made established decisions before attempting to use Deep Reinforcement Learning for autonomous decision-making. A therapy has total fractions f(r) fraction /dose b(r) as a function of time r with:

$$f(r_*) = f_0, \quad f(R) = 30, \; b(r) = \begin{cases} b_0, & 0 \le r \le r_* \\ b_1, & r_* \le r \le R \end{cases} \tag{9}$$

As shown in equation (9) where R is the time of accomplishing treatment with $0 < r_* < R$, r_* is the time for adaption, and f_0, b_0, b_1 are constants objects to the conditions

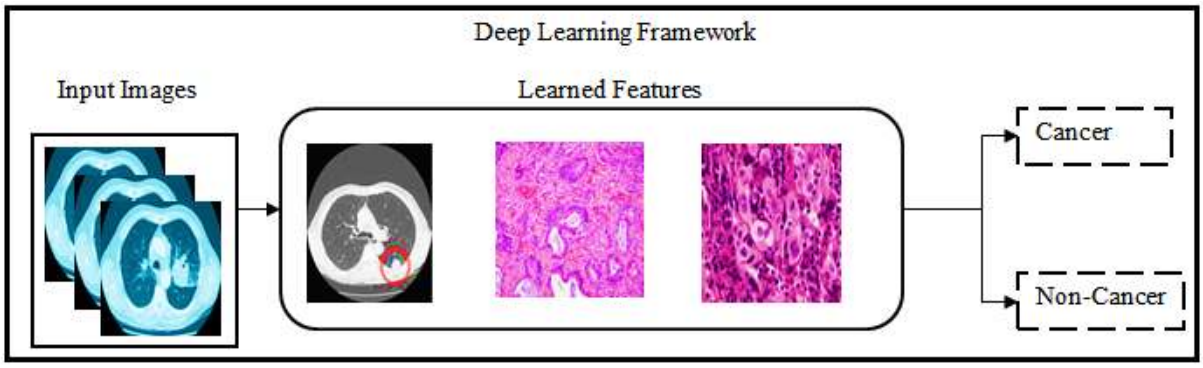

FIGURE 3. Training procedure of a deep learning method.

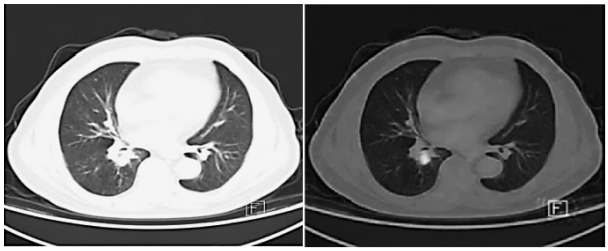

(a)Irregular mass with high lesion (b) Anterior Segment with lesion

FIGURE 4. Metabolic tumor volume.

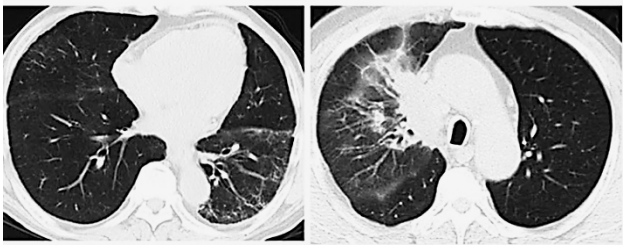

(a) CT of Emphysema Grade-0 (b) CT of Emphysema Grade-1

FIGURE 5. Radiation pneumonitis grade.

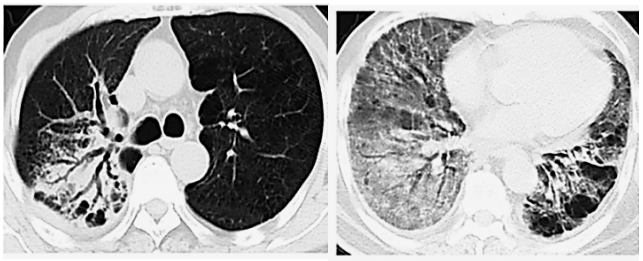

(a) CT of Emphysema Grade-2 (b) CT of Emphysema Grade-3

FIGURE 6. Radiation pneumonitis grade.

$b_0 \in [2.2, 2.9]H_z$, $b_1 = [2.9, 5.1]\ H_z$ and the total dose,

$$63H_z \leq b_0 f_0 + b_1(30 - f_0) \leq 86H_z \tag{10}$$

The rest of the dose is given for the target depends on avid mid-therapy defined through the metabolic tumor volume (MTV) as shown in the Figure.4.(a & b) The radiation will be given depends on pre-Computed Tomography. The protocol needs normal tissue complication probability (NTCP) of the lung to be maintained by $\leq$ 17.3% basis calculated by the LKB model.

$$NTCP\,(y) = \frac{1}{\sqrt{2\pi}} \int_{-\infty}^{y} e^{-\frac{v^2}{2}} dv \tag{11}$$

with

$$y = \frac{lung\ hEUD - TD_{50}}{n \cdot TD_{50}} \tag{12}$$

The clinical endpoint for lung normal tissue complication probability in the protocol,

$$\begin{aligned} &b_0 \cong 2, \quad b_1 \geq 2, \quad f_0 \cong 20, \quad R = 6\ weeks \\ &r_* \cong week\ 4 = \frac{2}{3} treatment \end{aligned} \tag{13}$$

Firstly, local discovery algorithms based on constraints using the Markov blankets has been used to select high-dimensional (297 candidates) variables that relate mostly to RP2/ LC. Then, to build a single Bayesian network from the attributes chosen for both the RP2 and the LC, with graphic learning algorithms. Finally, cross-validation has been used for determining and assessing nodes at Bayesian Network with the highest Area Under Curve value of joint prediction for LC and RP2. This procedure resulted in 9 selected features, including SNPs, cytokines, PET, and miRNA, which has been deemed to reflect the state variables as important predictors.

This conducts to describe the reward (15) as a trade-off between promoting better Local tumor Control and attempting to suppress radiation pneumonitis grade 0-3. The final word here is intended to obey with the provision of the clinical protocol for the radiation pneumonitis grade 0-1 as shown in the Figure.5 (a & b) risk likelihood not reach 17.3% and the radiation pneumonitis grade 2-3 as shown in the Figure.6 (a & b) risk likelihood not reach 19.3%. To establish

the state variable as following the equation (14),

$$w = (y_1, \ldots y_m) \in W \quad with\, m = 9 \tag{14}$$

To define the reward function $T(w, b) = T(w)$ depends on the LC (P^+) utility while corresponding the dose-escalation clinical protocol needs,

$$\begin{aligned} T(w) &= \frac{1}{2} prob(LC\,|w) \cdot (1 - prob(RP2\,|w)) \\ &\quad \cdot (1 + sgn(17.2\% - prob(RP2\,|w))), \\ sgn(y) &= \begin{cases} 1, & y > 0 \\ 0, & y = 0 \\ -1 & y < 0 \end{cases} \end{aligned} \tag{15}$$

As shown in equation (15) where $w \in W$, prob $(LC\,|w)$ is the conditional likelihood of determining LC after preserving state w, same for prob$(RP2\,|w)$.

In the mathematical model of Deep Q network, Q-function in equation (7) is stated to has the same form to (4) with a Deep Neural Network structure and weights Θ that should be finetuned for the best estimation of the actual Q-function:

$$P^{\Theta}_{DNN} : W \to T^{|B|} \; by \; P^{\Theta}_{DNN}(w) = \begin{pmatrix} P(w, b_1) \\ P(w, b_2) \\ \vdots \\ P(w, b_l) \end{pmatrix} \tag{16}$$

As shown in equation (16) where the outputs and inputs are modified to take benefit of the DL proficiencies rather than pursuing them literally (4).

This preparation has been carried out through state transitions and by two times (initial and during radiation therapy) (l = 0.1) with a sample size of dual as high as those of the patients.

$$\widetilde{Q}_{w_j^{(l)}, b_j^{(l)}}\left(w_j^{(l+1)}\right) = \widetilde{prob}\left(w_j^{(l+1)} \left| w_j^{(l)}, b_j^{(l)} \right.\right) \tag{17}$$

with $\left\{z_j = w_j^{(l+1)}\right\}$ worked as labels in the loss function.

$$L = \sum\nolimits_{l=0}^{1} \sum\nolimits_{j=1}^{M} \left\| z_{DNN}\left(w_j^{(l)}, b_j^{(l)}\right) - z \right\|^2 \tag{18}$$

As shown in the above equations where z_{DNN} is a set of Deep Neural Network classifiers to simulate $\widetilde{Q}$. The transition likelihood function of nine different attributes selected can be more accurately trained due to GAN created patient data. The radiotherapy artificial environmental z^j_{DNN} would be represented by a DNN Classifier ensemble with its inputs and outputs:

$$z^j_{DNN} : \{-1, 0, 1\}^9 \to -1, 0, 1\} \tag{19}$$

As shown in equation (19) where the cross-entropy loss function of multi-class detection has adopted for training,

$$L(\Theta) = -\frac{1}{M} \sum\nolimits_{j=1}^{M} \sum\nolimits_{l=1}^{L} z_j^{(l)} \log\left(\rho^{(l)}\left(\Theta \cdot x_j^{k-1}\right)\right) \tag{20}$$

In this regard, the likelihood transformation function approximation for producing adequate synthetic patient data from historical therapy plans using independent DNN and Generative Adversarial Nets. In an operational dose-escalation analysis with objective recompense functions, our proposed method has positively demonstrated.

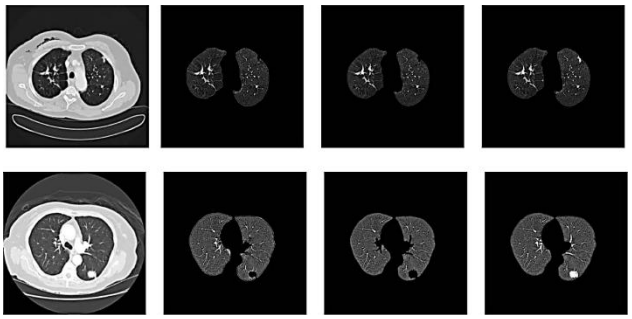

(a) (b) (c) (d)

FIGURE 7. Comparison of segmentation outcomes for all the grades (a) Computed Tomography images (b) segmentation established by region growing (c) Lung segmentation established by Modified K-means clustering algorithm (d) Lung segmentation established by AHHMM approach.

IV. RESULTS AND DISCUSSION

The findings of segmentation included nodules connecting to the inner wall and precise segmentation of the lung parenchyma. In the classification and detection of objects, efficient segmentation is very important. An efficient method of segmentation is developed based on the distribution of lung CT images by spatial pixel intensity. CT-images will simply remove pulmonary parenchyma in morphological operations; however, tissue around the lung can be included. Figure 7 shows the segmentation results comparison 7(a) shows the CT images 7(b) shows the segmentation established by region growing 7(c) shows the Lung segmentation established by Modified K-means clustering algorithm 7(d) shows the Lung segmentation established by AHHMM approach.

A. MEAN ACCURACY ANALYSIS

The suggested k-means lung segmentation, which offers 96% lung cancer segmentation, and only maintains this mean accuracy in low dose Computed Tomography images, and the same approaches are recommended for separating the lungs into high-resolution Computed Tomography images. The classifier accuracy can not be determined by the complete set of data set attributes. The measured value is compared with the extracted and trained features for cancer classification based on deep learning. Double time matching enhances the accuracy of prediction and decreases the failure rate efficiently. The mean accuracy of the classifier specifies how many samples has been correctly predicted by the total number of samples and is shown as follows. Figure 8 shows the mean accuracy ratio analysis of the proposed AHHMM method.

$$Mean\,Accuracy\,Ratio = \frac{True\,positive + True\,Negative}{Totalno\,of\,predictions} * 100 \tag{21}$$

TABLE 1. Mean accuracy analysis.

Methods	Image 1	Image 2	Image 3	Image 4	Image 5	Image 6	Image 7	Image 8	Image 9	Image 10
Double convolutional deep neural network (DCDNN)	**78.5**	**88.4**	**89.3**	**90.2**	**91.3**	**92.8**	**93.4**	**94.6**	**94.7**	**94.9**
Artificial Neural Network (ANN)	92.8	93.6	92.54	92.31	93.4	92.97	92.5	93.78	94.2	94.4
Deep Convolutional neural network (DCNN)	96.5	97	97.4	96.1	97.6	96.2	97.4	97.5	97.6	97.8
Improved profuse clustering technique and deep learning instantaneously trained neural network (IPCT-DLITNN)	97.2	97.5	97.1	97.8	97.9	97.45	97.9	98.01	97.9	98.2
Adaptive Hierarchical Heuristic Mathematical model (AHHMM)	98.09	98.4	98.2	98.4	98.6	98.1	98.5	98.2	98.8	98.9

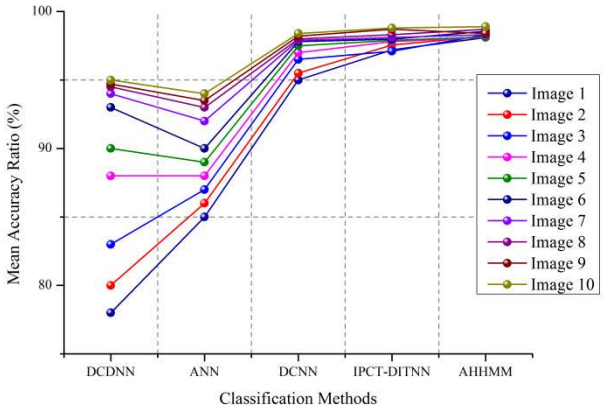

FIGURE 8. Mean accuracy ratio.

Table 1 shows the mean accuracy analysis of the proposed AHHMM method. Biopsy predicts lung cancer, it is rather difficult to maintain precision and accuracy. The CT scan is therefore done by the transmission of x-rays for the analysis of changes in the body. The technique of screening has helped to predict cancer of the lung, it is difficult to maintain an earlier recognition of large cell carcinoma and cancer detection.

B. DETERMINATION OF EFFICIENCY RATIO

The efficiency of the proposed AHHMM method evaluated in various aspects of recognition rate, misclassification ratio, precision, sensitivity, and accuracy. The high number of CT data has enabled us to use a moderate mini-batch size and to regulate training processes to achieve adequate speed and efficiency. In general, manual inspection is difficult to identify these quantitative image features, computerized methods can efficiently identify those features and our classifiers can be used effectively in routine practices. The DNN system is efficient and effective in classification. Figure 9 demonstrates the efficiency ratio of the AHHMM method.

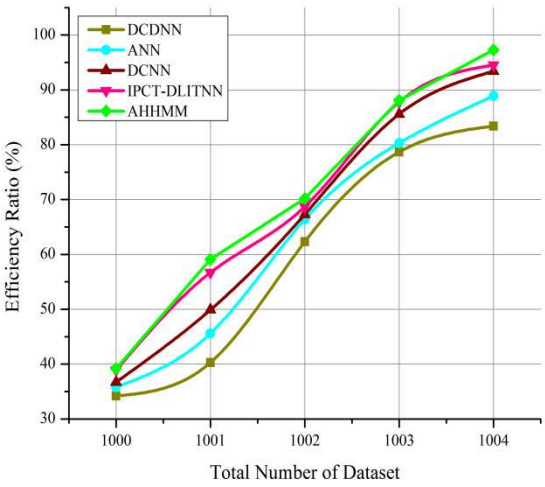

FIGURE 9. Efficiency ratio.

Table 2 shows the efficiency evaluation of the proposed AHHMM method. An effective algorithm has been developed to detect lung cancer and to forecast it using MATLAB, using

TABLE 2. Efficiency evaluation.

Total Number of Dataset	DCDNN	ANN	DCNN	IPCT-DLITNN	AHHMM
1000	34.2	35.8	36.7	38.9	39.2
1001	40.3	45.6	49.9	56.7	59.1
1002	62.3	66.4	67.3	68.7	70.2
1003	78.7	80.3	85.6	87.8	88.1
1004	83.4	88.9	93.4	94.5	97.3

image processing technology. Classification of multi-stage cancer has been used in lung diagnosis. This algorithm has been used to predict lung cancer. The algorithm tests the likelihood of lung cancer, if there is no cell affected by cancer in the input image. If the cells of cancer have been detected, search the algorithm for the correct stage such as the first, medium and final stages of cancer. The algorithm. Improving and segmenting images using several techniques before every stage of the classification process.

C. PROBABILITY OF SURVIVAL RATE

A relative survival rate is equivalent to the general population of people with the same cancer type and stage. The rate of survival depends on different treatments, cancer, and comorbidity. Cancer treatments are often very difficult to choose and must be based on experience, clinical processes, and comorbidities. Each of these variations will affect the decision of the doctor. When all the data available in the image are used by a deep network to predict survival, the collider is conditioned and thus a predictor of the treatment effect is made. An especially aggressive lung tumor may grow to a large extent, as can be seen with CT scans, leading to worse overall survival. In a simulation study of binarian treatment and a reliable outcome representing overall survival, the nodule size has been utilized and variance in radiodensity. Figure 10 shows the probability of survival rate.

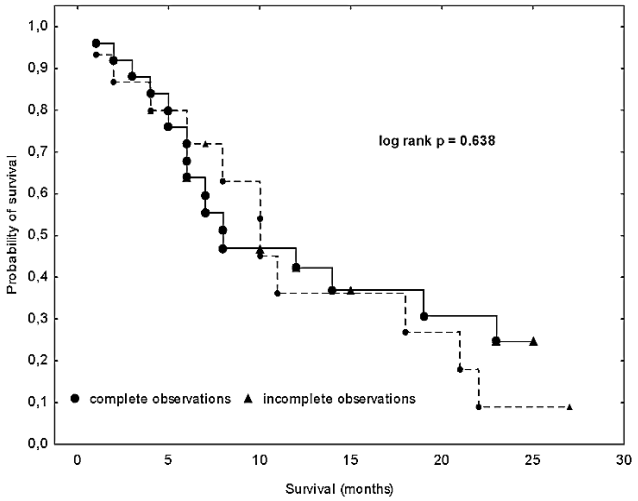

FIGURE 10. Probability of survival rate.

D. THE LOSS FUNCTION OF AHHMM

The training process has been carried on until convergence or overfitting has been tested through an increase in total loss on the self simulated validation of images different from the training set. All DNN parameters and final layer activations has been set after convergence. A new loss feature has been proposed to allow new knowledge to be acquired within control populations in environments with varying levels of risk. A huge number of sample data can efficiently enhance the training and accuracy of the NN, decrease the loss function and ultimately enhances the resilience of neural networks. Figure 11 shows the loss function of the AHHMM method.

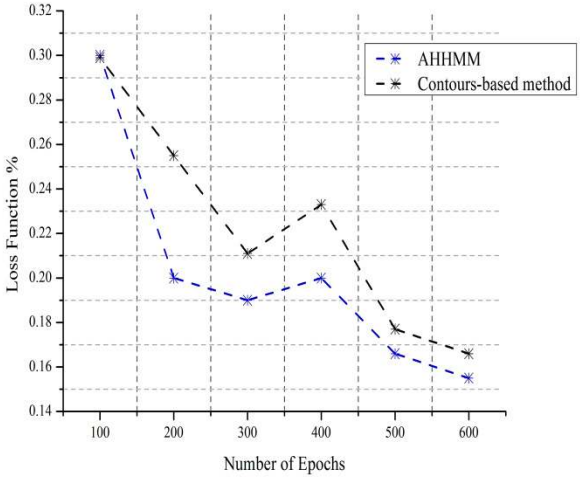

FIGURE 11. The loss function of AHHMM.

E. MISCLASSIFICATION RATIO

The misclassification ratio is known as error rate such as classifier which is not predictable properly. Data may not be correctly categorized in a non-linear setting. To decrease the misclassification rate, it minimizes the margin so that all of the vectors are classified in their corresponding space. In this case, it must increase the margin of the hyperplane. The error in the feature extraction comes primarily from two aspects: the restriction of the neighborhood size due to expected variance and the estimated error of the layer of convolution due to a mean deviation. Whereas pooling will every the first error and maintain more details on the picture context. Max pooling will decrease the error and maintain more data about texture. Figure 12 shows the misclassification ratio of the proposed AHHMM method.

$$Misclassification\ Ratio = \frac{False\ Positive + False\ Negative}{Totalno\ of\ predictions} * 100 \quad (22)$$

Based on above analysis, the deep learning assisted Adaptive Hierarchical Heuristic Mathematical Model (AHHMM) has better to efficiency to predict lung cancer on computed tomography images.

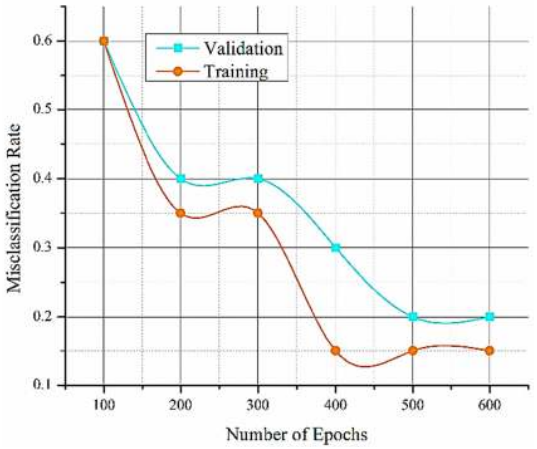

FIGURE 12. **Misclassification ratio.**

V. CONCLUSION AND FUTURE SCOPE

Lung cancer is a dangerous disease, and early-stage detection is therefore necessary. This paper presents deep learning assisted Adaptive Hierarchical Heuristic Mathematical Model (AHHMM) to predict lung cancer on computed tomography images. This paper uses the Modified K-means algorithm to pre-classify pictures into slices of images in the same image, where the DNN will concentrate on the image classification of images in similar images. The next thing is the convolution layer with filtered edges to scan for lung cancer thoroughly. Then, estimating the weighted mean function which replaces the pixel utilizing the cumulative distribution and likelihood distribution method improved the images quality. The injured portion has been segmented by a pixel-like value measurement after the image has been improved. Based on the similarity calculation, spectral-related features has been extracted. The proposed AHHMM system predicts computed tomography scanning images of lung cancer successfully. At the end of the system, you can say that the system is satisfying its desires. The findings of the evaluation showed that around 90% of the images has correctly identified. Such results show that DNN is useful in cyst diagnosis for classifying lung cancer. Hybridized Heuristic Mathematical Model will be implemented in future for predicting the lung cancer at earlier stage.

REFERENCES

[1] N. Coudray, P. S. Ocampo, T. Sakellaropoulos, N. Narula, M. Snuderl, D. Fenyö, A. L. Moreira, N. Razavian, and A. Tsirigos, "Classification and mutation prediction from non-small cell lung cancer histopathology images using deep learning," *Nature Med.*, vol. 24, no. 10, pp. 1559–1567, 2018.

[2] P. Gupta and A. K. Malhi, "Using deep learning to enhance head and neck cancer diagnosis and classification," in *Proc. IEEE Int. Conf. Syst., Comput., Autom. Netw. (ICSCAN)*, New York, NY, USA: ACM, vol. 28, Jul. 2018, pp. 1–7.

[3] Q. Song, L. Zhao, X. Luo, and X. Dou, "Using deep learning for classification of lung nodules on computed tomography images," *J. Healthcare Eng.*, vol. 2017, pp. 1–7, Aug. 2017.

[4] H. Xie, D. Yang, N. Sun, Z. Chen, and Y. Zhang, "Automated pulmonary nodule detection in CT images using deep convolutional neural networks," *Pattern Recognit.*, vol. 85, pp. 109–119, Jan. 2019.

[5] B. A. Skourt, A. El Hassani, and A. Majda, "Lung CT image segmentation using deep neural networks," *Procedia Comput. Sci.*, vol. 127, pp. 109–113, Jan. 2018.

[6] K. Kuan, M. Ravaut, G. Manek, H. Chen, J. Lin, B. Nazir, C. Chen, T. C. Howe, Z. Zeng, and V. Chandrasekhar, "Deep learning for lung cancer detection: Tackling the kaggle data science bowl 2017 challenge," 2017, *arXiv:1705.09435*. [Online]. Available: http://arxiv.org/abs/1705.09435

[7] F. Ciompi, K. Chung, S. J. van Riel, A. A. A. Setio, P. K. Gerke, C. Jacobs, E. T. Scholten, C. Schaefer-Prokop, M. M. W. Wille, A. Marchianò, U. Pastorino, M. Prokop, and B. van Ginneken, "Towards automatic pulmonary nodule management in lung cancer screening with deep learning," *Sci. Rep.*, vol. 7, no. 1, Jun. 2017, Art. no. 46479.

[8] Q. Wu and W. Zhao, "Small-cell lung cancer detection using a supervised machine learning algorithm," in *Proc. Int. Symp. Comput. Sci. Intell. Controls (ISCSIC)*, Oct. 2017, pp. 88–91.

[9] W. Alakwaa, M. Nassef, and A. Badr, "Lung cancer detection and classification with 3D convolutional neural network (3D-CNN)," *Lung Cancer*, vol. 8, no. 8, p. 409, 2017.

[10] C. Wang, A. Elazab, J. Wu, and Q. Hu, "Lung nodule classification using deep feature fusion in chest radiography," *Computerized Med. Imag. Graph.*, vol. 57, pp. 10–18, Apr. 2017.

[11] W. Sun, B. Zheng, and W. Qian, "Automatic feature learning using multichannel ROI based on deep structured algorithms for computerized lung cancer diagnosis," *Comput. Biol. Med.*, vol. 89, pp. 530–539, Oct. 2017.

[12] A. Masood, B. Sheng, P. Li, X. Hou, X. Wei, J. Qin, and D. Feng, "Computer-assisted decision support system in pulmonary cancer detection and stage classification on CT images," *J. Biomed. Informat.*, vol. 79, pp. 117–128, Mar. 2018.

[13] S. Bhatia, Y. Sinha, and L. Goel, "Lung cancer detection: A deep learning approach," in *Soft Computing for Problem Solving*. Singapore: Springer, 2019, pp. 699–705.

[14] D. Ardila, A. P. Kiraly, S. Bharadwaj, B. Choi, J. J. Reicher, L. Peng, D. Tse, M. Etemadi, W. Ye, G. Corrado, D. P. Naidich, and S. Shetty, "End-to-end lung cancer screening with three-dimensional deep learning on low-dose chest computed tomography," *Nature Med.*, vol. 25, no. 6, pp. 954–961, Jun. 2019.

[15] *Lungs Tumors and Nodules Segmentation With Deep Learning*. [Online]. Available: https://www.rsipvision.com/lung-nodules-segmentation/

[16] Y. Bar, I. Diamant, L. Wolf, S. Lieberman, E. Konen, and H. Greenspan, "Chest pathology detection using deep learning with non-medical training," in *Proc. IEEE 12th Int. Symp. Biomed. Imag. (ISBI)*, Apr. 2015, pp. 294–297.

[17] M. Schwyzer, D. A. Ferraro, U. J. Muehlematter, A. Curioni-Fontecedro, M. W. Huellner, G. K. von Schulthess, P. A. Kaufmann, I. A. Burger, and M. Messerli, "Automated detection of lung cancer at ultralow dose PET/CT by deep neural networks–initial results," *Lung Cancer*, vol. 126, pp. 170–173, Dec. 2018.

[18] S. L. Fernandes, V. P. Gurupur, H. Lin, and R. J. Martis, "A novel fusion approach for early lung cancer detection using computer aided diagnosis techniques," *J. Med. Imag. Health Informat.*, vol. 7, no. 8, pp. 1841–1850, Dec. 2017.

[19] N. Nasrullah, J. Sang, M. S. Alam, and H. Xiang, "Automated detection and classification for early stage lung cancer on CT images using deep learning," in *Proc. 30th Pattern Recognit. Tracking*, May 2019, Art. no. 109950.

[20] H. Jiang, H. Ma, W. Qian, M. Gao, and Y. Li, "An automatic detection system of lung nodule based on multigroup patch-based deep learning network," *IEEE J. Biomed. Health Informat.*, vol. 22, no. 4, pp. 1227–1237, Jul. 2018.

[21] S. K. Lakshmanaprabu, S. N. Mohanty, K. Shankar, N. Arunkumar, and G. Ramirez, "Optimal deep learning model for classification of lung cancer on CT images," *Future Gener. Comput. Syst.*, vol. 92, pp. 374–382, Mar. 2019.

[22] S. M. Salaken, A. Khosravi, A. Khatami, S. Nahavandi, and M. A. Hosen, "Lung cancer classification using deep learned features on low population dataset," in *Proc. IEEE 30th Can. Conf. Electr. Comput. Eng. (CCECE)*, Apr. 2017, pp. 1–5.

[23] R. Golan, C. Jacob, and J. Denzinger, "Lung nodule detection in CT images using deep convolutional neural networks," in *Proc. Int. Joint Conf. Neural Netw. (IJCNN)*, Jul. 2016, pp. 243–250.

[24] S. Trajanovski, D. Mavroeidis, C. Leon Swisher, B. G. Gebre, B. S. Veeling, R. Wiemker, T. Klinder, A. Tahmasebi, S. M. Regis, C. Wald, B. J. McKee, S. Flacke, H. MacMahon, and H. Pien, "Towards radiologist-level cancer risk assessment in CT lung screening using deep learning," 2018, *arXiv:1804.01901*. [Online]. Available: http://arxiv.org/abs/1804.01901

[25] S. Shen, S. X. Han, D. R. Aberle, A. A. Bui, and W. Hsu, "An interpretable deep hierarchical semantic convolutional neural network for lung nodule malignancy classification," *Expert Syst. Appl.*, vol. 128, pp. 84–95, Aug. 2019.
[26] K. Pawełczyk, M. Kawulok, J. Nalepa, M. P. Hayball, S. J. McQuaid, V. Prakash, and B. Ganeshan, "Towards detecting high-uptake lesions from lung CT scans using deep learning," in *Proc. Int. Conf. Image Anal. Process.* Cham, Switzerland: Springer, Sep. 2017, pp. 310–320.
[27] G. Jakimovski and D. Davcev, "Using double convolution neural network for lung cancer stage detection," *Appl. Sci.*, vol. 9, no. 3, p. 427, 2019.
[28] I. M. Nasser and S. S. Abu-Naser, "Lung cancer detection using artificial neural network," *Int. J. Eng. Inf. Syst.*, vol. 3, no. 3, pp. 17–23, 2019
[29] A. Teramoto, T. Tsukamoto, Y. Kiriyama, and H. Fujita, "Automated classification of lung cancer types from cytological images using deep convolutional neural networks," *BioMed Res. Int.*, vol. 2017, pp. 1–6, Aug. 2017.
[30] P. M. Shakeel, M. A. Burhanuddin, and M. I. Desa, "Lung cancer detection from CT image using improved profuse clustering and deep learning instantaneously trained neural networks," *Measurement*, vol. 145, pp. 702–712, Oct. 2019.

HENG YU was born in Henan, China, in 1984. He received the bachelor's and master's degrees from Henan University, in 2008 and 2011, respectively. He is currently working as a Lecturer with the School of Information Engineering, Pingdingshan University, Henan. He has published nine articles, one of which has been indexed by EI. His research interests are digital image processing and machine learning.

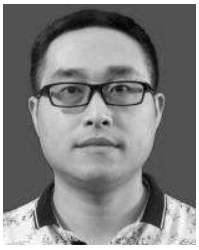

ZHIQING ZHOU was born in Zhejiang, China, in 1978. He received the bachelor's and master's degrees from Central China Normal University, in 2002 and 2007, respectively. He is currently working as a Lecturer with the School of Information Engineering, Pingdingshan University, Henan. His major fields of study include the Internet of Things and machine vision.

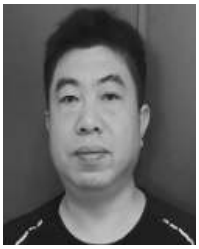

QIMING WANG was born in Lushan, Henan, China, in 1980. He received the master's degree in computer technology from Xidian University, China, in 2009. He is currently working as an Assistant Professor with the School of Information Engineering, Pingdingshan University, Pingdingshan, Henan. His major fields of study include software engineering and networking algorithms.